

DIGITAL FILTERS USED FOR DIGITAL FEEDBACK SYSTEM AT CERL

F. QIU[#], S. MICHIZONO, T. MIURA, H. KATAGIRI, D. ARAKAWA, T. MATSUMOTO, IBARAKI,305-0801, JAPAN.

Abstract

As a test facility for the future KEK 3-GeV energy recovery linac (ERL) project, the compact ERL (cERL) features three two-cell cavities for the injector and two nine-cell cavities for the main linac. Digital low-level radio frequency (LLRF) systems have been developed to realize highly accurate RF control. In order to reduce the influence of clock jitter and to suppress the parasitic modes in the multi-cell cavities, we have developed several types of digital filters, including a first-order IIR filter, a fourth-order conjugate poles IIR filter and a notch filter. Furthermore, to design a more effective and robust controller (such as an H-infinite controller, or repetitive controller), we need to acquire more detailed system knowledge. This knowledge can be gained by using modern system identification methods. In this paper, we present the latest applications in the LLRF systems of the cERL.

down-converted to a 10-MHz intermediate frequency (IF) signal and then processed by digital signal processing (DSP) algorithms that are implemented in an FPGA. The main functions of the algorithms include in-phase and quadrature (I/Q) detection, amplitude/phase (A/P) calibration, digital filter, feedback (FB) control, and feed forward (FF) control. The processed signal is then up-converted to an RF signal again to drive the power source of each cavity. Detailed information about this digital platform can be found in [7].

INTRODUCTION

The compact energy recovery linac (cERL) is a prototype machine that was developed for the planned light source 3-GeV ERL project at KEK [1]. It is a superconducting (SC) project and is operated in the continuous wave (CW) mode. Three two-cell cavities and two nine-cell cavities were installed in the injector and main linac (ML), respectively. To achieve a low-emittance beam, the RF field fluctuation should be maintained to less than 0.1% (in amplitude) and 0.1° (in phase). The challenging requirements are satisfied by using μ TCA-based digital low-level RF (LLRF) systems [2].

To suppress the parasitic modes in the nine-cell cavities of the ML in the cERL, a high-order IIR filter was proposed and implemented in the cERL. As a comparison, a second-order notch filter was also developed and applied in the system [3].

A system model is required in order to design the more effective controlling applications. Such as H-infinite multi-input multi-output (MIMO) control [4], disturbance observer controls (DOBs) [5], and repetitive controls (RCs) [6]. Modern system identification techniques provide a method for determining the mathematical model of the system.

This paper focuses on the development of a high-order IIR filter for parasitic mode suppression. Experiments on system identification in the CW mode are presented as well.

LLRF SYSTEM

The schematic diagram of the LLRF system for cERL is shown in Fig.1. The 1.3-GHz cavity probe signal is

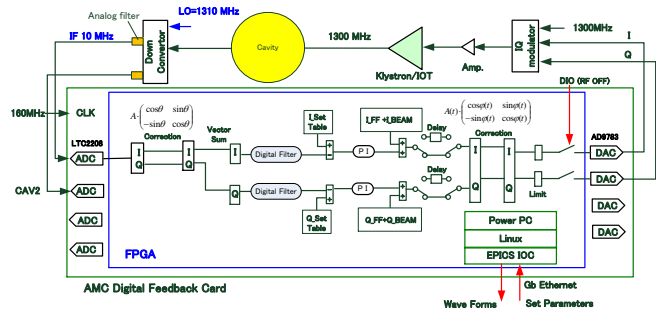


Figure 1: Schematic of the LLRF system in the cERL.

NINE-CELL CAVITY IN MAIN LINAC

Two nine-cell L-band superconducting cavities were installed in the ML of the cERL [8]. The nine-cell cavity hosts a normal RF mode and eight different parasitic modes; only the π mode is used for the beam acceleration. The parasitic modes, especially the so-called $8\pi/9$ mode limit the feedback loop gains. For the cavity of the ML1, the location of π mode and parasitic modes is shown in Fig. 2.

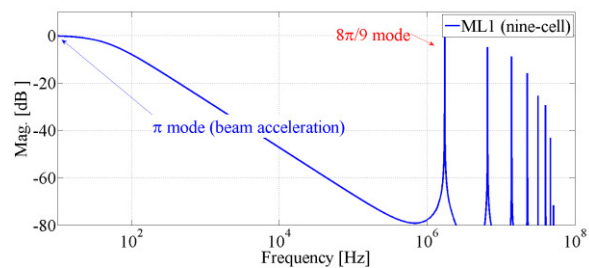


Figure 2: Bode plot of the nine-cell cavity in the ML1. The nearest parasitic mode ($8\pi/9$ mode) is located around 1.7 MHz from the π mode.

HIGH ORDER FILTER

Applying digital filters is an effective means to remove the parasitic modes. In the previous LLRF system, an IIR-type filter, which has a difference equation, as shown in (1) was selected as the main filter. It is the simplest IIR filter with only one real-pole. The filter bandwidth is proportional to the adjustable parameter α .

[#]qiufeng@post.kek.jp

$$y(n) = \alpha \cdot x(n) + (1 - \alpha) \cdot y(n-1), \quad \alpha \ll 1 \quad (1)$$

For a sufficient gain margin, 60 dB attenuation is required for the $8\pi/9$ mode (and other parasitic modes); otherwise, there is a risk of closed-loop instability. This goal can be achieved by reducing the bandwidth of the first order IIR filter to 2 kHz; however, the phase delay in such a narrow bandwidth filter is very large, and thus the loop gain will be limited to a very small value.

To improve the roll-off, a high-order filter that has a pair of conjugate poles is proposed. Fig. 3 compares the pole-zero plot of the previous first order IIR filter and the proposed conjugate poles filter.

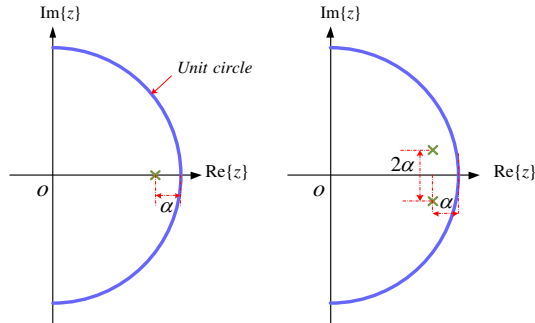


Figure 3: Pole-zero plot of the previous IIR filter (left) and proposed conjugate-poles filter (right). The proposed filter has a pair of conjugate poles $p_{1,2} = (1 - \alpha) \pm j\alpha$.

According to Fig. 3, the proposed conjugate-poles IIR filter in difference equation form is given by

$$y(n) = \sqrt{2}\alpha \cdot x(n) + a_1 \cdot y(n-1) + a_2 \cdot y(n-2) \quad (2)$$

where $a_1 = 2(1 - \alpha)$ and $a_2 = -(1 - \alpha)^2 - \alpha^2$.

Fig. 4 compares the bode diagram of different filters, in the frequency range of interest ($f < 100$ kHz), the phase delay of the proposed filter (indicated by the red curve) is significantly lower than the previous one (indicated by the blue curve). In our design, two conjugate-poles filter are connected in serials to improve the roll-off.

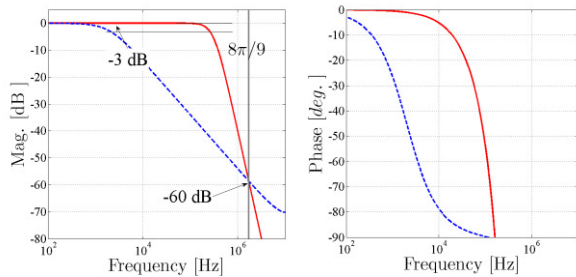


Figure 4: Bode plot (left: magnitude, right: phase) of different filters. The proposed filter (red) with 60 dB attenuation at 1.7 MHz ($8\pi/9$ mode) will maintain a 250 kHz bandwidth, whereas the previous one (blue) with the same attenuation provides only a 2-kHz bandwidth.

Figure 5 has shown the comparison of the closed-loop regulation with and without the filter. At the beginning, we operated the system without filter and gradually increased the loop gain. The closed loop oscillated immediately owing to the parasitic modes. The maximum

loop gain was limited to less than 1. The oscillation disappeared after applying the proposed filter. The system worked well even with a high loop gain of up to 400.

Another candidate for suppressing the parasitic modes is notch filter. The study in [3] shows approach to control the nine-cell cavity with notch filter. To compare with the proposed conjugate-poles IIR filter, the present research also applied a notch filter (of the same type in [3]) for removing the $8\pi/9$ mode.

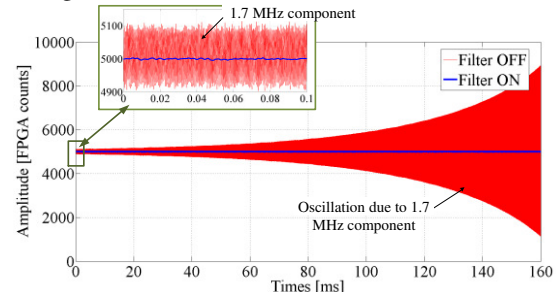


Figure 5: Closed-loop operation with and without filter. In the case without filter (red line), even a very low gain ($K_P = 1$) would result in system oscillation because of the existence of the $8\pi/9$ mode.

Table 1 compares the previous first-order filter, the proposed high-order filter, and a notch filter. Both the proposed filter and the notch filter perform well for high-gain operation (the maximum gain can be up to 400 for both cases). However, compared with the notch filter, the proposed type in (2) is much easier to implement and consumes fewer FPGA resources.

Based on these analyses, we ultimately selected the proposed conjugate poles filter as the main filter in the LLRF system of the ML. In the cERL beam commissioning, the RF stabilities under the optimum proportional gain $K_P = 150$ (evaluated by a gain-scanning experiment, see [2] and [8]), were 0.012% rms in amplitude and 0.013° rms in phase. These values satisfied the requirements of the cERL operation. The performance result of the LLRF system in the beam commissioning are presented in [8].

Table 1: Comparison of different filters at the cERL

Filter Type	Att. @ $8\pi/9$	$G_{optimal}$	$G_{critical}$
No filter	0	/	1
First Order	60 dB	/	<10
Conjugate	60 dB	150	~400
Notch	>60 dB	150	~400

SYSTEM IDENTIFICATION

The PI controller is the main controller of the current LLRF system in the cERL. To improve system performance, feedback gains were surveyed and optimized [2]. However, in order to further enhance the system capabilities such as the robustness and disturbance

constraint, more advanced control methods are required. Approaches include the H-infinite control, disturbance observer control, and repetitive control. The system model is indispensable in all of these approaches [4]-[6]. System identification provides a convenient method to determine the mathematical model of the system.

The research in [4] gives the procedure for the system identification in detail; however, the applications in [4] were implemented in pulse mode. For the CW operation in the cERL, one of the most difficult problems is generating the noise source (which is the input signal for the system identification) in real time.

A Pseudo-noise (PN) sequence is a good noise source for the system identification. This sequence is periodic with a potentially large cycle time and is therefore deterministic [9]. Even if the PN sequence is not perfectly random, it has similar statistical properties with real sampled white noise. The best advantage of the PN sequence is that its implementation in an FPGA is extremely simple. The main components are shift registers and exclusive-or (XOR) gates. Detailed information about PN sequences can be found in [9]. As an illustration, Fig. 6 has shows the block diagram of a PN sequence generator.

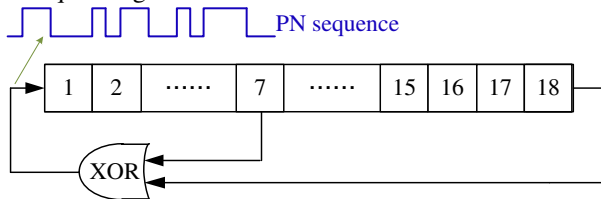


Figure 6: Block diagram of a PN sequence generator. The main components are shifter registers and one XOR gate.

After inserting the PN generator presented above into the FF table of the LLRF system in the cERL, we performed the system identification experiment. Fig. 7 shows the open-loop Bode plot of the identified mathematical model (the fourth-order black box model), including both the on-diagonal and cross components. Fig. 8 compares the model output and the measured response (located after the digital filter in Fig. 1). These results show that the dynamic behavior of the system can be precisely described by the model.

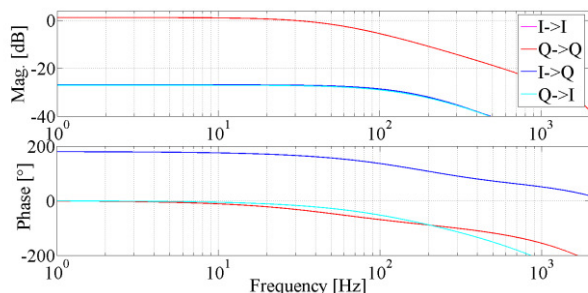


Figure 7: Bode plot of the open loop LLRF system in the ML1. Both on-diagonal and cross channels are presented.

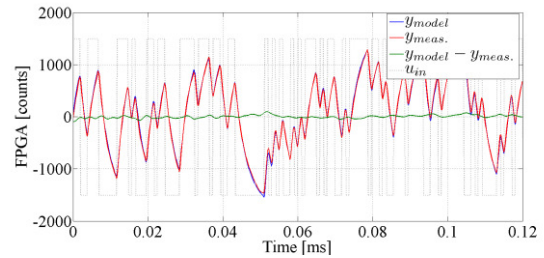


Figure 8: Comparison of the measured output (red) and identified model output (blue) of the I channel.

SUMMARY

The cERL system was constructed and beam commissioning was carried out. In the nine-cell cavities of the ML, because of the parasitic modes, high gain is not possible in the closed loop operation. The proposed conjugate poles IIR filter was implemented to solve this problem. During the beam commissioning, all the parasitic modes were suppressed successfully, and a high gain of up to 400 was achieved. The RF stabilities under optimum gains ($KP = 100$) satisfied our requirements. Furthermore, to further improve the LLRF control system; we performed the system identification experiment in the CW mode with a PN sequence generator. Results show that the identified model can accurately represent the system.

REFERENCES

- [1] S. Sakanaka et al., “The First Beam recirculation and beam tuning in the compact ERL at KEK”, LINAC14, Geneva, Sep., 2014.
- [2] F. Qiu et al., “Evaluation of the superconducting LLRF system at cERL in KEK”, IPAC’13, Shanghai, May 2013.
- [3] C. Schmidt et al., “Precision Regulation of RF fields with MIMO Controllers and Cavity-based Notch filters, IPAC’13, Shanghai, May 2013, FRXBB201
- [4] C. Schmidt, “RF System Modeling and Controller Design for the European XFEL”, Ph.D. thesis, Hamburg, 2010.
- [5] J. Carl et al., “Disturbance Observer and Feed Forward Design for a High-Speed Direct-Drive Positioning Table”, IEEE Trans. Contr. Syst. Technol. 7(5), 513-526 (1999).
- [6] X. Chen et al., “New Repetitive Control with Improved Steady-state Performance and Accelerated Transient”, IEEE Trans. Contr. Syst. Technol. 22(2), 664-675 (2014).
- [7] T. Miura et al., “Low-Level LLRF system for cERL”, IPAC’10, Kyoto, May 2010, TUPEA048.
- [8] F. Qiu et al., “Performance of the Digital LLRF System at the cERL”, IPAC’14, Dresden, June, 2014.
- [9] S. Malviya et al., “Implementation of Pseudo-Noise Sequence Generator on FPGA Using Verilog”, International Journal of Electronic and Electrical Engineering. 7(8),887-892 (2014)